Effects of Partial Mixing and Confinement on Detonation Wave Characteristics and RDE Mode of Operation

Shikha C. Redhal, Minwook Chang, Jason R. Burr, and Ken H. Yu
University of Maryland
College Park, Maryland, USA

1 Abstract

Experimental investigation is performed to quantify various dynamic parameters associated with detonation waves in a partially confined channel such as that occurring in rotating detonation engine (RDE) combustors. Although the complexity of the transient injection, evolving mixing and the cyclic processes contributes to the difficulty in properly predicting the RDE operating characteristics such as its stability and performance, the main problem has been the lack of quantitative information on the characteristic detonation parameters in the relevant, partially-confined geometry. In this study, simultaneous measurements of pressure, CH*-chemiluminescence, and shadowgraph visualizations are made for five different cases of detonation waves, that resulted over transversely injected methane-oxygen reactant flows in a linear model detonation engine configuration. The five cases consisted of three different levels of shock-flame coupling and two different fill heights, representing different levels of partial mixing and partial confinement due to boundary walls. From the detailed measurements, we can not only obtain the characteristic time scales associated with local pressure relaxation, chemical reaction period, and any induction delays between the shock and flame processes, but it was also possible to analyze the stability of various wave modes of operation in a model RDE.

2 Experimental Setup

Experiments were conducted using an extended Linear Model Detonation Engine (eLMDE) shown in Fig. 1. This rig simulates experimentally an unwrapped configuration of a RDE combustor. All the dimensions of the experimental setup are normalized by the recessed tube diameter d, 0.1 inch. The setup consists of an array of 48 transverse reactant jets placed inside a linear open channel, 3.6d wide, through which a detonation wave propagates. The injector consists of a recessed tube, which is 11.25d in depth and the reactants impinge at the base of the tube at 10d from the injection plane. Confinement of reactant species is provided on the sides by the quartz windows and below by the injection plane. A timed arrival of a detonation wave into the injector flowfield is controlled using a pre-detonator connected into the test section from the left side. Independent solenoid control for each reactant allows for control over the height of the partially premixed reactant layer just prior to detonation wave transit.

Correspondence to: sredhal@umd.edu

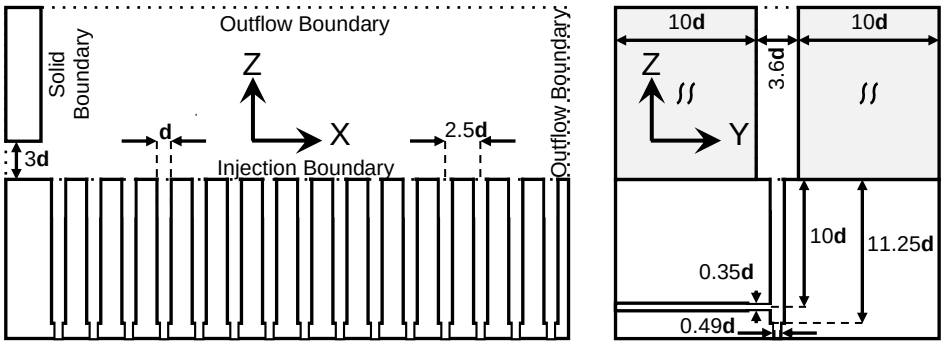

Figure 1: Cross-section of LMDE channel in the X-Z (left) and Y-Z (right) planes, with X-Y-Z forming right-handed coordinate system. Dimensions normalized by injection tube diameter, d

The test conditions and the observed wave speeds for the cases discussed in this paper are given in Table 1. Five different cases are considered in this paper, and they are characterized on the basis of the detonation wave speed as well as the state of coupling between the lead shock wave and the flame fronts that can be observed from the flow visualization. These cases are to represent various types of detonation wave structures, which may be observed in a practical RDE. The corresponding shadowgraph images of the detonation wave propagating from left to right are shown in Fig 2 for each case.

Table 1: Different cases of detonation wave strength

Case No.	Wave or Flow Characteristics	Measured Detonation Wave Speed
1	Decoupled Wave	710 ± 100 m/s
2	Weakly Coupled	1900 ± 200 m/s
3	Strongly Coupled	2100 ± 150m/s
4	Lower Fill Height	2060 ± 100 m/s
5	Greater Fill Height	2300 ± 100 m/s

Measurements for wall pressure and CH* chemiluminescence associated with detonation wave passage can be taken simultaneously using a dynamic pressure transducer (PCB) and a photomultiplier tube with a 430nm band pass filter, respectively. Typical sampling was done at 500kHz or higher. High-speed flow visualization images were obtained using both schlieren and shadowgraph techniques, typically conducted at 30 kHz or higher framing rate.

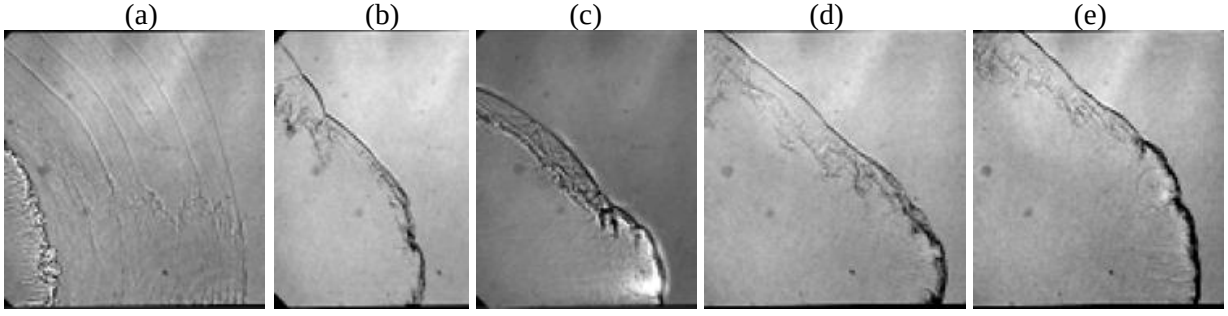

Figure 2. Shadowgraph images representing each case: (a) decoupled wave, (b) weakly coupled, (c) strongly coupled, (d) lower fill height, and (e) higher fill height

3 Experimental Results and Discussion

Experiments were conducted with methane and oxygen as reactants in the eLMDE. While the average flow rates of each gas were set for the stoichiometric ratio, the actual balance of methane-oxygen mixture inside the combustor at the exact time of detonation wave arrival is determined by the timing of the pre-detonator as well as the injector valve timings that control the local mixedness. As a result, variations in the observed wave characteristics can be obtained by adjusting the relative timing

between reactant valves and the arrival of a detonation wave from the pre-detonator within a micro second level.

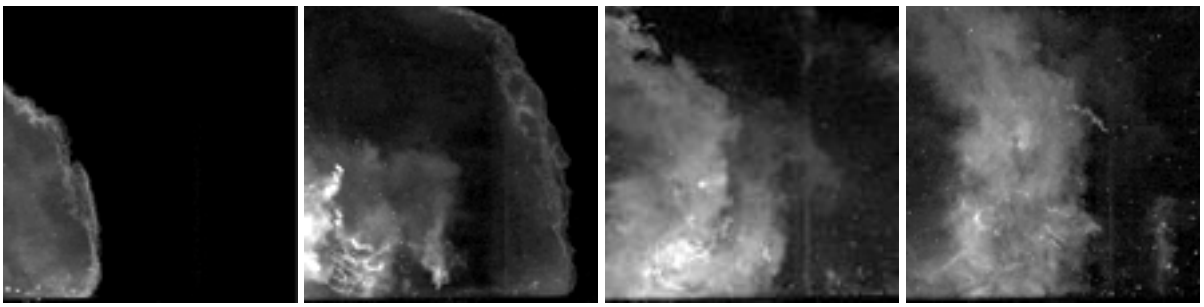

Figure 3. Luminescence associated with decoupled detonation wave, each taken at 100 µsec apart.

When the shock wave and the flame front are completely separated as in Case 1, the entire structure is referred to as a "decoupled" detonation wave. The shock wave is propagating ahead of the respective flame front with a clear separation between the wave fronts, and the separation distance is typically more than one injector spacing. Figure 3 shows the natural luminescence from the separated flames propagating in the wake of the shock wave. It can be observed from the images that the reaction zone is no longer concentrated in the wave front but rather it is distributed over a range of injectors. Each image was taken at 100 µsec apart as the wave structure propagates from left to right in the channel. The corresponding CH* chemiluminescence signal and the dynamic component of the pressure signal are shown in the Fig 4a. It can be seen clearly that there is a measurable time lag between the pressure and chemiluminescence signal indicating a decoupled detonation wave.

Figure 4b and 4c show the pressure and the CH* chemiluminescence for cases 2 and 3 respectively. Case 2 corresponds to a "weakly-coupled" detonation wave case. Compared to the decoupled case, there is a much stronger coupling between the pressure and the flame front as indicated by the chemiluminescence and pressure signals. Nevertheless, the two signals are not totally synchronized as the chemiluminescence signal is often trailing the pressure signal by up to a few microseconds. Additionally, the coupling between the smaller peaks of the pressure and PMT after the detonation wave transit can be seen along with

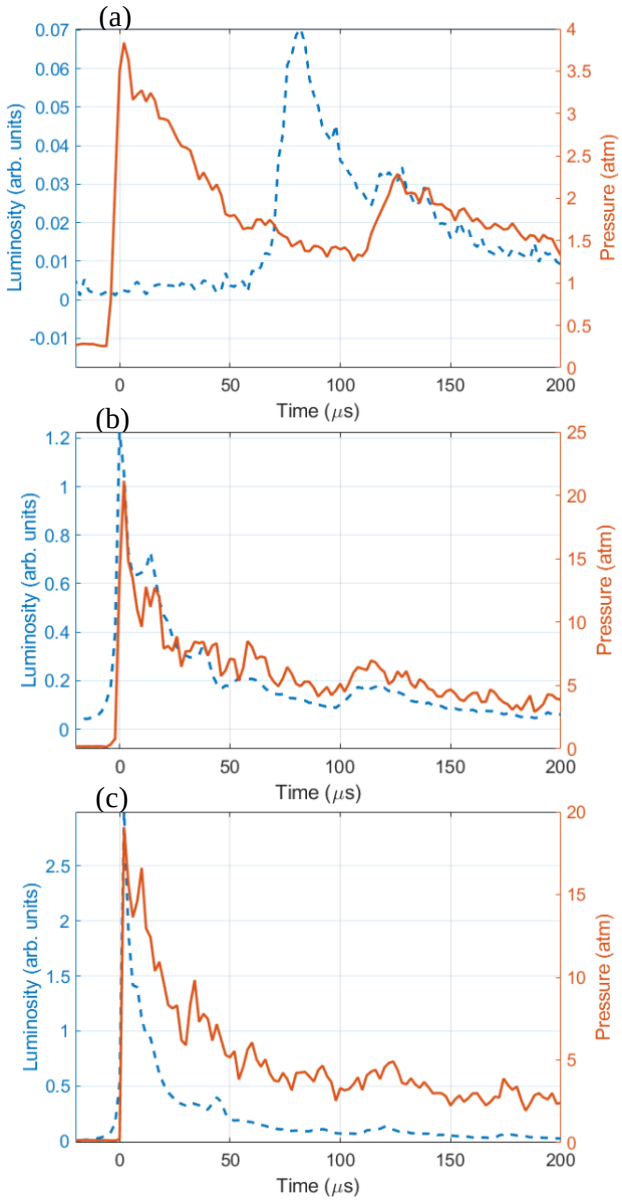

Figure 4: Luminosity measured with PMT and Pressure data for (a) Case 1 (b) Case 2 (c) Case 3

the coupling between the rise times. The correlation between the two signals can help us understand the deflagration of the unburnt reactants and reflected shocks in the detonation channel. Case 3 corresponds to a strongly coupled detonation case where most of the heat release is confined in the flame front. In Fig. 4c, the peaks for the pressure and the chemiluminescence signals are synchronized

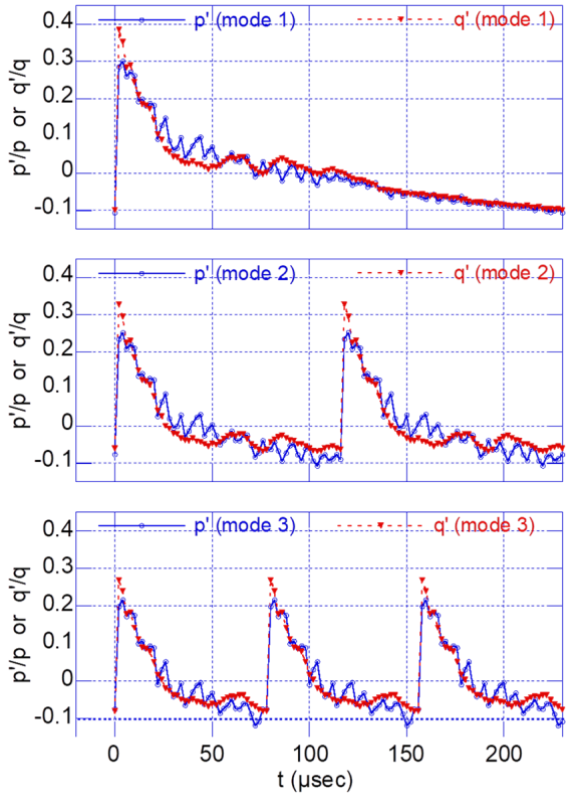

Figure 5: Weakly-coupled detonation waves (Case 2) modeled inside a 4-inch RDE, and the resulting pressure-heat release fluctuation coupling

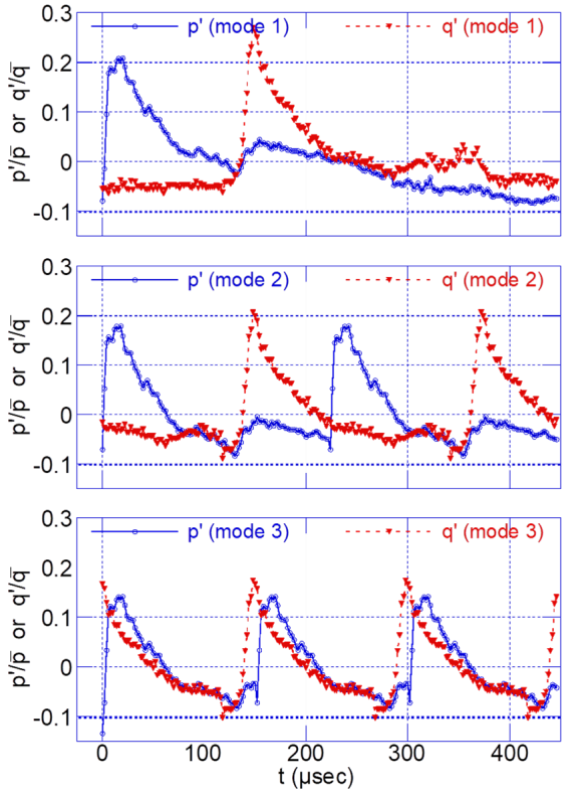

Figure 6: Decoupled detonation waves (Case 1) modeled inside a 4-inch RDE, and the resulting pressure-heat release fluctuation coupling

showing that it is a classic detonation wave. Comparing figure 4a, 4b and 4c, it can be observed that the half width of the chemiluminescence signal is reduced as the coupling becomes stronger indicating that the heat release also gets confined to a smaller area for driving the detonation wave forward.

If similar waves as characterized in the eLMDE channel were operating inside an RDE combustor, it would be possible to analyze their stability characteristics using the Rayleigh energy criterion for pressure-heat release fluctuation coupling. For example, in a 4-inch diameter RDE, if coupled-detonation waves as characterized in Case 2 were produced, various scenarios of multiple waves trapped inside the combustor would be possible as shown in Fig. 5. Due to the coupled nature of pressure maximum and heat release maximum, the resulting pressure fluctuations (p') and heat release fluctuations (q') would always be in phase and their interaction should produce positive energy feedback according to the Rayleigh criterion. On the other hand, decoupled-detonation waves of Case 1 would only produce positive interaction when their separation distance or the phase delay should satisfy a certain criteria as dictated by the Rayleigh criterion. Again, some scenarios of multiple waves are illustrated in Fig. 6. For this case, the second higher harmonic case (Mode 3) would result in nearly in-phase pressure and heat release fluctuations and it would likely be the dominant mode of RDE operation.

Rayleigh index calculations for various modes for this RDE model are plotted in Fig. 7 for these two types of detonation waves. The results confirm that the fundamental mode (Mode 1) would have the highest amount of acoustic energy production in the case of the coupled detonation wave, while the three-wave mode (Mode 3) would most likely be the dominant mode in the case of decoupled detonation wave.

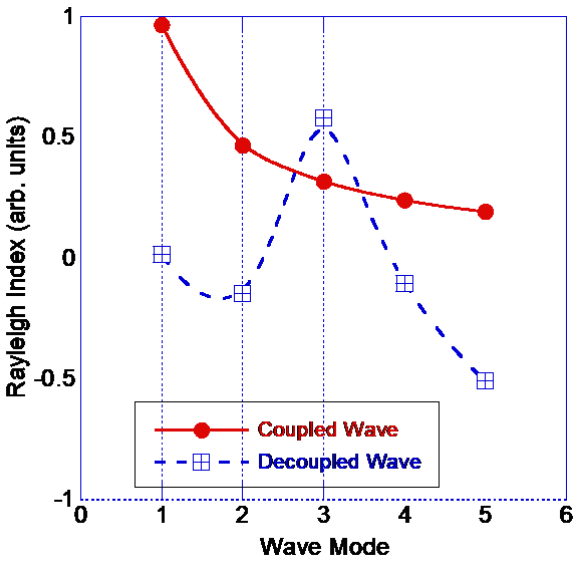

Figure 7: Rayleigh index for a 4-inch model RDE with various wave modes

Effects of reactants fill height were also investigated. Table 2 shows the detailed boundary conditions for the case 4 and case 5. Both the cases are compared in terms of the degree of confinement and the ratio between the cell size of the methane-oxygen detonation to the hydraulic diameter of fill height of the fresh reactants in the detonation channel. The lower fill height results in a smaller level of reactant confinement as the unconfined area on the top side becomes relatively more significant compared to the confined area of each side.

Table 2. Effect of injection fill height

Case No	Characteristic Flow	Injection Fill Height, (H_{jet})	Area Confinement Ratio, $A_{wall}/(A_{wall}+A_{open})$	Fill Height/Cell Size ($H_{jet}/\lambda_{detonation}$)
4	Lower fill height	20d	0.928	6.1
5	Greater fill height	25d	0.941	7.7

From Case 4 to Case 5, the injection fill height was increased by 25%. Although the case with the greater fill height resulted in a slight increase in the average wave speed, the resulting detonation waves were fully coupled in both cases and relatively little qualitative difference was observed. Also, for both cases, the relative confinement ratio was greater than 0.92 and the fill height in terms of maximum detonation cell size was greater than 6.

The chemiluminescence images of both cases are shown in Fig. 8a and 8b. It can be observed that the lower fill height detonation have less number of the triple points compared to the higher fill height. As a result, the detonation in Case 4 can be more sensitive to the local mixing in the channel leading to some runs of an unstable detonation. On the contrary, typical runs in Case 5 appear to be more stable and more repeatable. In Fig. 8a at t=τ+33 μs, the triple point is observed at the pressure transducer location resulting in a strong pressure and chemiluminescence signal.

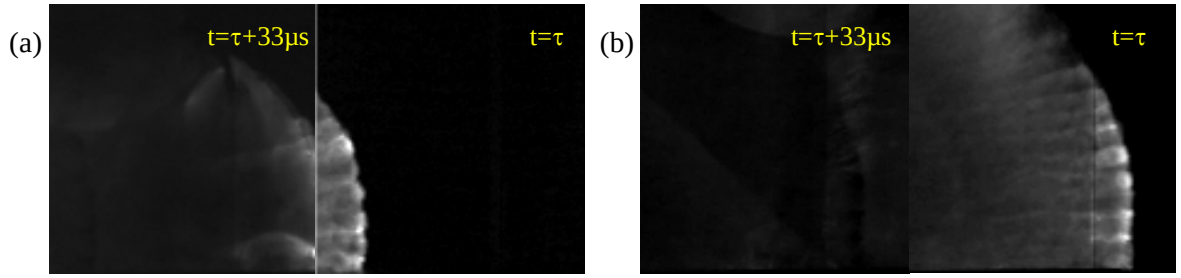

Figure 8. CH* chemiluminescence images corresponding to (a) Case 4, and (b) Case 5

Fig. 9 shows the plot of the average full width half maximum Δt of the PMT chemiluminescence signal. It is observed from the plot that the strongly coupled detonation cases have smaller Δt and standard deviation as compared to the weakly coupled and uncoupled detonation cases. It shows that the strongly coupled cases have CH* concentration in a thinner region while weakly coupled case have wide spread of the CH* chemiluminescence. This thickness corresponds to the flame thickness of the detonation wave and the results agree with the chemiluminescence images.

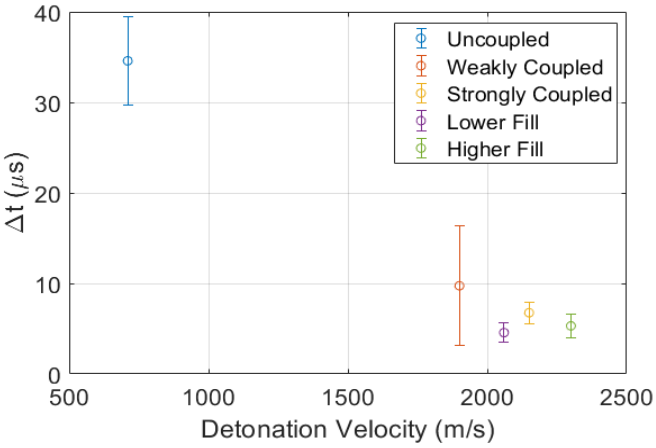

Figure 9: Average full half width maximum of the PMT chemiluminescence signal for all the cases

4 Concluding Remarks

We investigated various types of detonation waves that may occur in typical RDE combustor flowfields and experimentally characterized the pressure and the heat release fluctuations associated with those waves. The detailed characteristics and relative phase information were used to perform stability analysis for various numbers of waves that may be fitted into a model RDE combustor. The results show that both strongly and weakly coupled detonation waves are likely to be stable in all number of waves. On the other hand, decoupled detonation waves exhibit a dominant mode which provide ideal positive interaction between the pressure peak produced by the shock waves running ahead of the flame fronts and the heat release from the prior waves. The decoupled CH4-O2 detonation wave we examined would produce a stable operation with a three-wave modes inside a 4-inch diameter model RDE.

It was also shown that the case with a lower degree of confinement led to a smaller number of the triple points in the detonation wave front, which resulted in a less stable mode of operation. Both the degree of partial confinement and the ratio of confinement diameter to the characteristic detonation cell size would likely affect the detonation wave stability characteristics, but more study is needed before drawing a definitive conclusion.

References

[1] Burr, J. R., & Yu, K., "Experimental characterization of RDE combustor flowfield using linear channel," Proceedings of the Combustion Institute, 37(3), 3471-3478 (2019).

[2] Burr, J. R., & Yu, K., "Characterization of CH4-O2 detonation in unwrapped RDE channel combustor," In AIAA Propulsion and Energy 2019 Forum (p. 4215) (2019).

[3] Clayton, R. M., and Rogero, R. S., "Experimental Measurements on a Rotating Detonation-Like Wave Observed During Liquid Rocket Resonant Combustion," NASA TR 32-788, JPL/Caltech, Pasadena, CA, (1965).

[4] Nicholls, J., Cullen, R., and Ragland, K. "Feasibility studies of a rotating detonation wave rocket motor," Journal of Spacecraft and Rockets, 3(6), pp.893-898, (1966).

[5] Adamson, T. C., and Olsson, G. R., "Performance Analysis of a Rotating Detonation Wave Rocket Engine," Astronautica Acta, 13(4), pp.405–415, (1967).

[6] Kindracki, J., Wolanski, P., and Gut, Z., "Experimental Research on the Rotating Detonation in Gaseous Fuels–Oxygen Mixtures," Shock Waves, 21(2), pp.75-84, (2011).